Electronic Spectroscopy of Jet-Cooled 1,2′-Binaphthyl

Fangtong Zhang, Ondrej Votava,† Anthony R. Lacey, and Scott H. Kable*

School of Chemistry, University of Sydney, Sydney, NSW, 2006, Australia

Received: January 9, 2001

The electronic spectroscopy of jet-cooled 1,2′-binaphthyl has been examined by laser-induced fluorescence spectroscopy. Many medium length progressions were observed in two active vibrations with frequencies $\nu_A' = 35.1$ cm^{-1} and $\nu_B' = 53.5$ cm^{-1} assigned as the torsion and out-of-plane wag between the two naphthalene moieties, respectively. Two other low-frequency vibrations were measured: $\nu_C' = 60.6$ cm^{-1} and $\nu_D' = 138.1$ cm^{-1}. These are also likely to involve inter-ring motion, possibly an in-plane wag for ν_C and an antisymmetric inter-ring motion for ν_D, although a low-frequency naphthalene ring vibration is also possible. The electronic origin transition was not observed because of a very weak Franck−Condon factor with the ground state. However, a Franck−Condon analysis provided an estimate of the origin transition at $T_{00} = 30\,828.2$ cm^{-1}. Progressions in both ν_A and ν_B are harmonic up to 13 quanta for ν_A and 5 quanta for ν_B. Therefore, the barrier for interconversion between the cis and trans conformers of 1,2′-binaphthyl must be much higher than the 500 cm^{-1} of harmonic vibrations measured here. A diffuse band, about 800 cm^{-1} higher in energy, was assigned to the $S_2 \leftarrow S_0$ transition. Previous semiempirical calculations predicted the electronic energy of the S_1 state and the magnitude of the naphthalene dimer splitting quite well. However, the calculations placed the interconversion barrier through 90° to be as low as 300 cm^{-1}. The Franck−Condon analysis also provided a change in equilibrium conformation angle of 18° upon electronic excitation, again in disagreement with calculations, which predict essentially no change in equilibrium torsional angle between the S_0, S_1, and S_2 states.

I. Introduction

The electronic spectroscopy and molecular structure of biaryl molecules, which are two aromatic rings systems combined by a single carbon−carbon bond, has been the subject of numerous investigations over several decades.[1−11] The interest in such studies has been largely focused on the torsional angle between the two aromatic ring systems. The equilibrium torsional angle, and the shape of the torsional potential is very sensitive to several factors: steric interference between the aromatic moieties, the electronic structure of either aromatic ring system, and the environment. Therefore, in similar molecules the conformation can be quite different. Even within the same molecule the equilibrium structure can change markedly upon electronic excitation or upon changing the environment. For example, in the prototypical biaryl molecule, biphenyl, the ground-state structure is planar in the solid state, whereas in the gas phase, it has a twisted structure with an angle between the rings of 42°. In the gas phase, the structure becomes planar again in the lowest excited state (S_1).[1,2]

Binaphthyl is the second simplest of the biaryl group of molecules and has received some attention in the past.[8,10,12−20] There are three isomers of binaphthyl: namely 1,1′-, 1,2′-, and 2,2′-binaphthyl depending on the location of the C−C′ linkage (see inset to Figure 1 for 1,2′-binaphthyl structures). Among these, the symmetric compounds 1,1′-binaphthyl (1,1′-BN) and 2,2′-binaphthyl (2,2′-BN) have been studied in some detail. The solution spectrum and gas-phase spectrum in a supersonic free jet have been reported for both species.[5,19−21] Semiempirical calculations have also been performed to elucidate the nature of the lowest several excited electronic states and to calculate the torsional potential, including the equilibrium structure and the barriers between conformers.[17,22,23]

A summary of previous results for biaryl molecules reveals that there is a competition between the resonance interaction between the aryl π-systems, which favors a planar structure of the rings, and the steric hindrance which promotes more orthogonal structures. BNs provide an excellent example in this regard. 1,1′-BN is the most sterically hindered of the BNs. The equilibrium structure in both S_0 and S_1 states places the two naphthalene structures almost perpendicular to each other.[5,15,19,21] Its spectrum, both in solution and gas phase, therefore resembles that of the naphthalene monomer.[5,19] On the other hand, 2,2′-BN is the least hindered. The ring systems are only 30° from planar in the S_0 state and completely planar in the S_1 state.[20,23] There is a considerable stabilization energy in this conformation and the spectrum is distinctively different from the parent naphthalene.[5,20]

The energy of the S_1-S_0 transition of 1,2′-BN in solution lies between 1,1′- and 2,2′-BN.[5,8] Semiempirical calculations agree that the conformation angle of the ring systems in 1,2′-BN is intermediate between 1,1′-BN and 2,2′-BN (∼55° from planar in both S_0 and S_1 states).[4,24,25] However, the gas-phase spectrum of 1,2′-BN has not been recorded, and hence, the competition between steric hindrance and π resonance stabilization has not been examined experimentally to compare with these calculations, which are now more than a decade old. The semiempirical calculations performed quite well for 1,1′-BN but only moderately well for 2,2′-BN (where π-resonance is more important).[19,20,22,23] Our aim here is to complete the experimental data

* To whom correspondence should be addressed. Email: s.kable@chem.usyd.edu.au.

† Current address: J. Heyrovsky Institute of Physical Chemistry, Dolejskova 3, 18223 Praha 8, Czech Republic.

10.1021/jp0101110 CCC: $20.00
Published on Web 05/04/2001

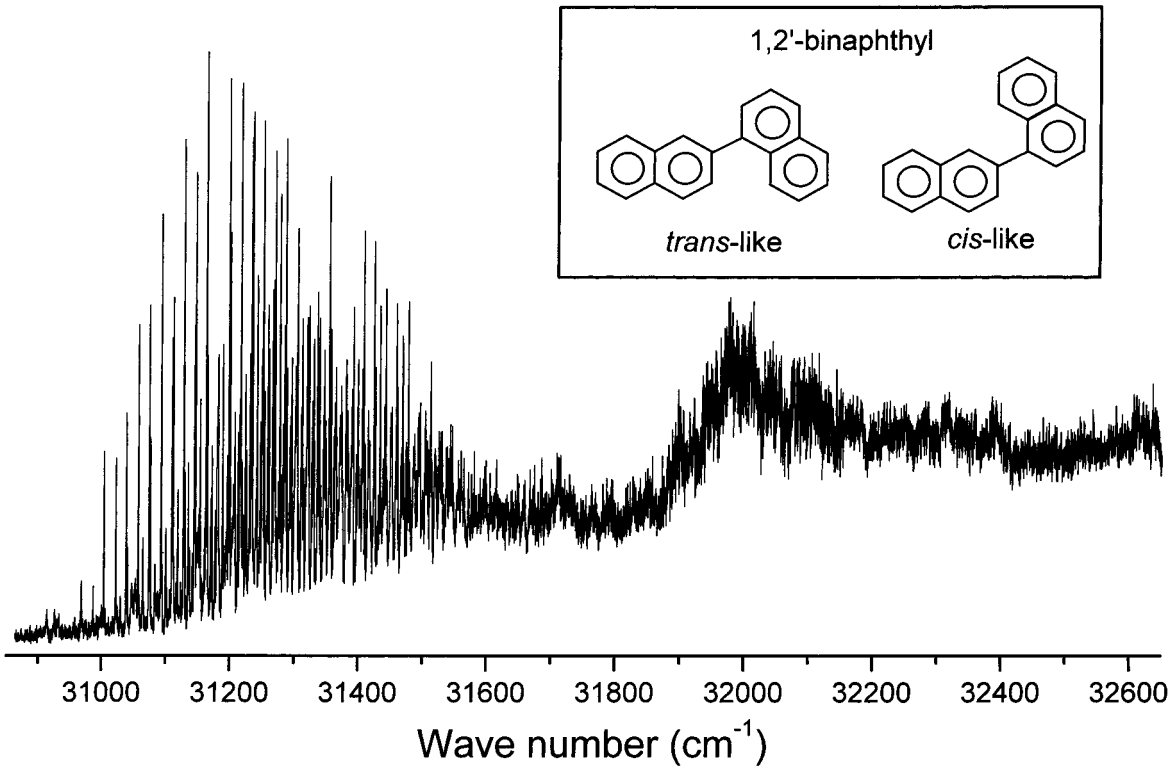

Figure 1. Low resolution LIF spectrum of 1,2′-BN showing the structured S_1-S_0 transition centered at 31200 cm^{-1} and the diffuse S_2-S_0 transition at 32 000 cm^{-1}.

set for the BN series and also to examine whether the conclusions from older semiempirical theory need to be updated across the series of three BN isomers.

In this work, we report the laser-induced fluorescence excitation spectrum of 1,2′-BN that has been cooled in a supersonic free jet expansion. Assignment of the vibrational structure leads to an estimate of the change in conformational angle upon electronic excitation and provides experimental information on the potential energy surface for twisting about the central C−C′ bond. This information will provide a stringent test for existing theory.

II. Experimental Section

In most regards, these experiments were performed in the same way as our previous experiments on 2,2′-binaphthyl.[20] Our description here is therefore brief. 1,2′-BN was supplied by Kodak and used as received. The sample was encased in a stainless steel in-line sintered filter holder (Nupro), which was mounted directly behind a General Valve Series 9 pulsed nozzle with a 0.5 mm orifice. The sample holder was heated to 100−110 °C using Nichrome wire to achieve sufficient sample vapor pressure in the expansion. The nozzle was heated to 110−120 °C also using Nichrome wire in a MACOR heating sleeve to inhibit condensation of 1,2′-BN molecules in the orifice. The temperatures of both the sample holder and the pulsed nozzle were monitored by 100 Ω platinum resistance thermometers.

Helium carrier gas was passed through the sample at pressures varying between 1 and 6 atm, although typically at 3 atm. The nozzle was pulsed at a repetition rate of 10 Hz, and the whole system was synchronized with the laser by a Stanford DG-535 digital delay generator. The vacuum chamber was kept at a stagnation pressure of below 10^{-6} mbar, rising to 2×10^{-4} mbar with the nozzle pulsing. This pressure was maintained by a water baffled Varian VHS-6 diffusion pump backed with an Alcatel 2033 rotary pump.

An excimer pumped dye laser system (Lambda Physik Lextra-200 excimer and LPD-3001e dye laser) was used in this experiment. The beam from the dye laser intersected the free jet expansion approximately 10 mm downstream from the nozzle. Two laser dyes were required to scan the 1,2′-BN spectrum. C-540A in ethanol provided light in the range 280−303 nm and DCM in methanol produced light in the range 302−335 nm, both after doubling in a KDP crystal. Fluorescence from 1,2′-BN molecules was collected with a photomultiplier (EMI 9789QB) via a monochromator (Spex Minimate). The fluorescence signal was averaged by a SRS-250 gated integrator and boxcar averager and interfaced to a personal computer. Laser power was monitored with a photodiode and dye cuvette for normalization of the spectrum.

III. Results

A low resolution laser-induced fluorescence (LIF) spectrum of 1,2′-BN in the range 30 800 to 32 650 cm^{-1} is presented in Figure 1. This spectrum is a combination of several scans because of the necessity to change dye and recalibrate the doubling crystal over this range. Two main features are evident in the spectrum. First, at lower energy is a region that includes several long progressions, which will be described in detail below. The second feature, toward higher energy, is a region of fluorescence with little structure. The peak of this broad band is at 32 000 cm^{-1}, approximately 800 cm^{-1} higher in energy than the sharply structured region. Further high- resolution scans were performed in the broad region but failed to find any meaningful structure.

Figure 2 shows a higher resolution LIF spectrum of the low energy region (first 500 cm^{-1}). A regular structure is very pronounced. Most of the structure in the spectrum can be assigned as progressions in two vibrations, one with a frequency of about 35 cm^{-1} (called ν_A) and the other with a frequency of about 53 cm^{-1} (called ν_B). Up to 13 quanta of ν_A and 5 quanta

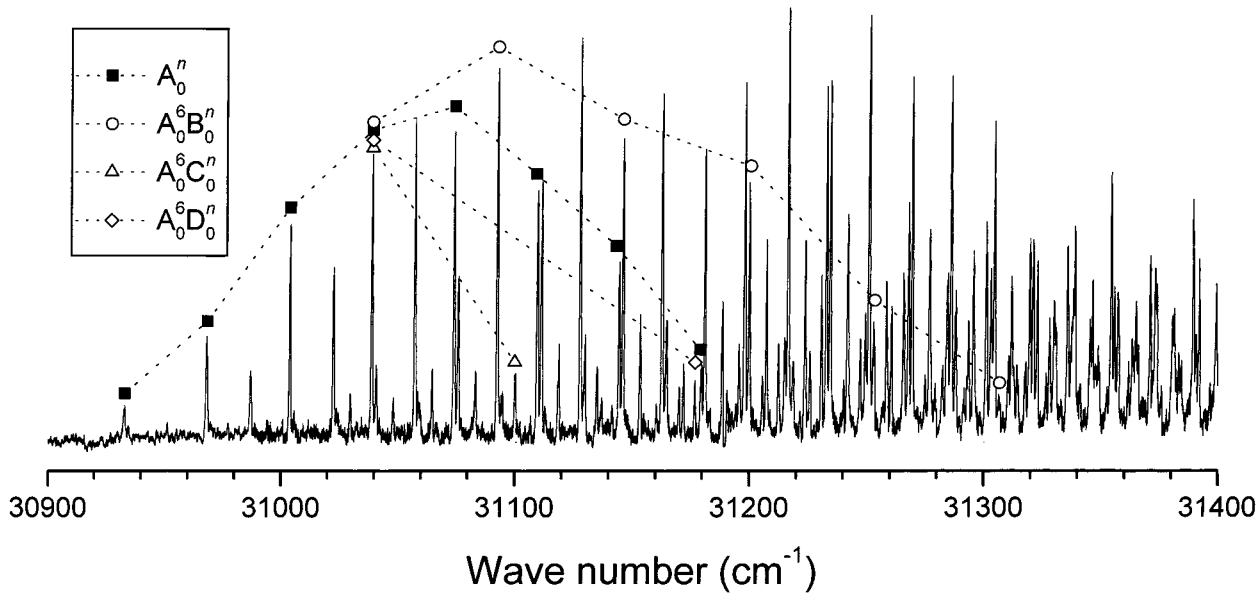

Figure 2. Higher resolution LIF spectrum of the S_1-S_0 transition of 1,2′-BN.

TABLE 1: Deslandres Table Showing the Observed Transitions Involving the Two Progression Forming Modes, ν_A and ν_B[a]

	$\upsilon_B = 0$		1		2		3		4		5
$\upsilon_A = 0$	**(30828.2)**[b]						**30988.6**				
							(35.1)				
1							**31023.7**				
							(35.4)				
2			**30951.1**	(54.4)	**31005.5**	(53.6)	**31059.1**				
			(35.6)		(35.3)		(35.6)				
3	**30933.0**	(53.7)	**30986.7**	(54.1)	**31040.8**	(53.9)	**31094.7**				
	(35.4)		(35.9)		(35.3)		(35.2)				
4	**30968.4**	(54.2)	**31022.6**	(53.5)	**31076.1**	(53.8)	**31129.9**	(53.7)	**31183.6**		
	(35.5)		(34.9)		(35.4)		(34.8)		(35.1)		
5	**31003.9**	(53.6)	**31057.5**	(54.0)	**31111.5**	(53.2)	**31164.7**	(54.0)	**31218.7**		
	(35.3)		(35.3)		(34.6)		(35.4)		(34.7)		
6	**31039.2**	(53.6)	**31092.8**	(53.3)	**31146.1**	(54.0)	**31200.1**	(53.3)	**31253.4**	(53.0)	**31306.4**
	(35.2)		(35.2)		(35.3)		(34.7)		(34.8)		(34.8)
7	**31074.4**	(53.6)	**31128.0**	(53.4)	**31181.4**	(53.4)	**31234.8**	(53.4)	**31288.2**	(53.0)	**31341.2**
	(35.3)		(34.9)		(35.2)		(34.8)		(34.6)		(34.7)
8	**31109.7**	(53.2)	**31162.9**	(53.7)	**31216.6**	(53.0)	**31269.6**	(53.2)	**31322.8**		**31375.9**
	(34.9)		(35.4)		(34.7)		(35.1)		(34.3)		(34.7)
9	**31144.6**	(53.7)	**31198.3**	(53.0)	**31251.3**	(53.4)	**31304.7**	(52.4)	**31357.1**	(53.5)	**31410.6**
	(34.9)		(34.8)		(35.1)		(34.2)		(34.9)		(34.4)
10	**31179.5**	(53.6)	**31233.1**	(53.3)	**31286.4**	(52.5)	**31338.9**	(53.1)	**31392.0**	(53.0)	**31445.0**
			(35.1)		(34.8)				(34.4)		(34.5)
11			**31268.2**	(53.0)	**31321.2**				**31426.4**	(53.1)	**31479.5**
			(35.1)		(35.9)				(34.6)		(34.3)
12			**31303.3**	(53.8)	**31357.1**				**31461.0**	(52.8)	**31513.8**
			(34.9)		(34.9)				(35.0)		
13			**31338.2**	(53.8)	**31392.0**				**31496.0**		

[a] The values in parentheses are the first differences in the frequencies of the vibrations either to each side, or above and below. [b] Extrapolated from other transitions in the table.

of ν_B have been assigned. A Deslandres table for these two Franck−Condon active modes is shown in Table 1. The first difference in the frequencies of neighboring progression members are shown in parentheses. Both sets of first differences reveal that the vibrations A and B are essentially harmonic. The average value across all A progressions in Table 1 provides $\nu_A' = 35.1$ cm^{-1}, whereas the B progressions provide $\nu_B' = 53.5$ cm^{-1}.

The remaining progressions in Figure 2 result from short progressions in two further modes, labeled ν_C and ν_D. Only one member of each of these progressions was observed, upon which were built the ubiquitous progressions in ν_A and ν_B. These assignments and frequencies are summarized in Table 2, which provide $\nu_C' = 60.6$ cm^{-1} and $\nu_D' = 138.1$ cm^{-1}.

The assignment of quantum numbers to ν_B, ν_C, and ν_D was straightforward because the transitions with zero quanta in these modes were Franck−Condon active. For example, one progression in each of these modes is indicated in Figure 2. The peak with four symbols has the assignment A_0^6, i.e., involving zero quanta in vibrational modes B, C, or D. The assignment in terms of these three modes is secure because there is no peak to the red of A_0^6 with a frequency spacing of 53.5, 60.6, or 138.1 cm^{-1}. Assignment of the υ_A quantum numbers was more problematic because the Franck−Condon intensity for the 0_0^0 transition is weak. In Figure 2 one progression in ν_A is shown as the solid square symbols. The first peak is fairly weak and it is reasonable to ask whether a peak 35 cm^{-1} to the red of

TABLE 2: Observed Transitions Involving ν_C and ν_D[a]

	$A_0^n C_0^1$	$A_0^n B_0^1 C_0^1$	$A_0^n B_0^2 C_0^1$	$A_0^n B_0^3 C_0^1$	$A_0^n D_0^1$	$A_0^n B_0^1 D_0^1$	$A_0^n B_0^2 D_0^1$	$A_0^n B_0^3 D_0^1$
$n = 0$								
1		30977.3						
2		31012.5						
3	30994.1	31048.1					31179.4	
4	31029.5	31083.3	31137.1	31190.7	31106.5	31160.6	31215.0	
5	31064.7	31188.8	31172.2	31226.0	31141.6	31195.9	31249.7	
6	31100.0	31153.6	31207.4	31260.8	31177.0	31230.9	31284.7	
7	31135.2	31188.8	31242.1	31295.8	31212.5	31266.1	31319.6	31373.2
8	31170.2	31223.8	31277.0	31330.0	31247.6	31301.3	31354.3	31408.2
9	31205.4	31258.6	31311.9	31364.9	31282.5	31335.9	31389.5	31442.8
10	31240.4	31293.5	31346.5	31399.5	31317.8	31371.3	31424.3	31477.5
11	31275.2	31328.2	31381.2	31434.0	31352.8	31406.3	31459.0	31512.0
12		31363.0	31415.7	31468.8		31440.9	31494.0	
13			31450.2	31504.3				

[a] Each of these modes forms a false origin for numerous progressions in ν_A and ν_B.

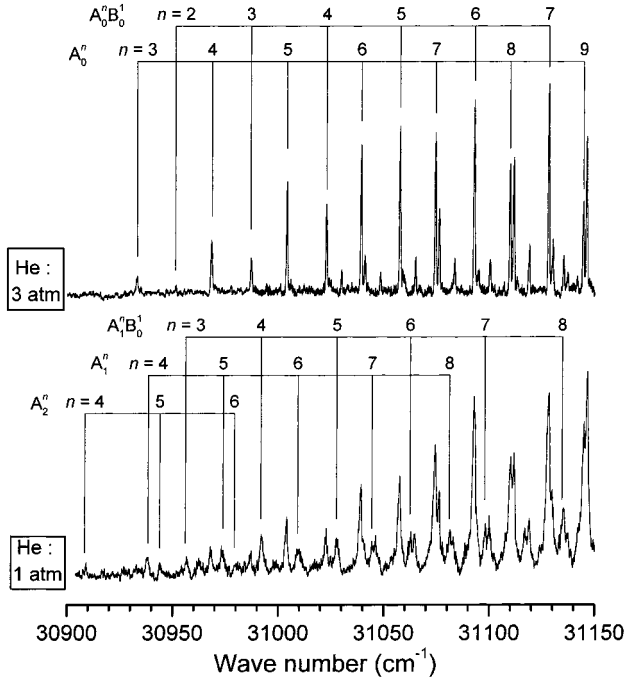

Figure 3. LIF spectra of 1,2′-BN under cold (He: 3 atm) and warm (He: 1 atm) jet conditions to accentuate the assignment of hot band features.

this first assigned peak would be observed above the noise. To be more certain in our assignment of ν_A quantum numbers we performed a Franck−Condon (FC) analysis of this vibration. We also remeasured the LIF spectrum under warmer jet conditions to try and observe hot band activity that might lead to assignment of the ground-state frequency ν_A'', which is valuable for the FC analysis (see below).

A. Hot Bands. In a supersonic jet, the degree of vibrational and rotational cooling depends on the carrier gas backing pressure. A higher backing pressure reduces the mole fraction of sample and increases the collision frequency, both of which contribute to a lower final temperature. Thus, by lowering the backing pressure, we seek peaks that were absent in the colder spectrum, and hence would be assigned as hot bands.

Figure 3 shows a region of the 1,2′-BN LIF spectrum under two different backing pressure conditions. The upper panel shows the spectrum taken with relatively high He pressure (3 atm). Here we focus on the ν_A and ν_B energy levels. The two cold progressions are the A_0^n and $A_0^n B_0^1$ progressions. In low He backing pressure (∼1 atm), three new short progressions were found. These progressions are assigned as hot bands because their intensity distribution is quite different from the cold transitions, and they disappeared when the He pressure was increased. The progressions are assigned as A_1^n, $A_1^n B_0^1$, and A_2^n. Two of the progressions are assigned as arising from population in the energy level with one quantum of ν_A''. A_1^{n+1} is shifted about $+4.5$ cm^{-1} from the corresponding cold progression, A_0^n, and $A_1^{n+1} B_0^1$ is likewise shifted about $+4.5$ cm^{-1} from $A_0^n B_0^1$. The third progression, A_2^{n+2}, is displaced a further ∼4.5 cm^{-1} from A_1^{n+1}. The sequence spacing for ν_A ($\nu_A' - \nu_A'' \approx 4.5$ cm^{-1}) and the excited-state frequency, ν_A', therefore provides an estimate of $\nu_A'' = 30.5$ cm^{-1}. This is consistent with the trend among biaryl molecules (including biphenyl,[1,2] 1,1′-BN[19,22] and 2,2′-BN[20,23]) to favor more planar conformations in the excited state than in the ground state. The closer the conformation is to planar, the greater is the double bond character in the C−C′ bond, which in turn provides a larger force constant for the inter-ring motion. Thus, the excited-state vibrational frequency is often greater than that of the ground state.

B. Franck−Condon Analysis of ν_A and ν_B. As discussed above, the progression marked by solid squares in Figure 2 involves purely ν_A. The intensity distribution of the members in this progression varies smoothly and symmetrically each side of a maximum, which occurs near 31 100 cm^{-1}. The relative intensity of all labeled peaks in Figure 2 was the same for a variety of He pressures, hence they are all believed to be cold bands.

The Deslandres table demonstrates that the potential energy function of this vibrational mode in the excited state is harmonic. On the basis of this, we have performed a harmonic one-dimensional Franck−Condon analysis to assist in locating the electronic origin in the spectrum of 1,2′-BN. This analysis treats vibrations in both the ground and excited electronic states as harmonic. Though we do not have sufficient information regarding the ground electronic state, all the progressions involved originate in $v'' = 0$, therefore anharmonic effects are not likely to be important.

A recursion relation (derived from the harmonic oscillator recursion relations) involving two parameters is used to calculate the FC overlap integral for each transition in the progression.[26] The first parameter, D, is related to the change in normal coordinate between the ground and excited electronic states. The second parameter, δ, is related to ground and excited torsional frequencies by $\delta = (\nu''/\nu')^{1/2}$, which in our case, is $(30.5/35)^{1/2} = 0.934$.

The upper panel of Figure 4 shows the intensity distribution for the origin progression. To model the experimental intensity

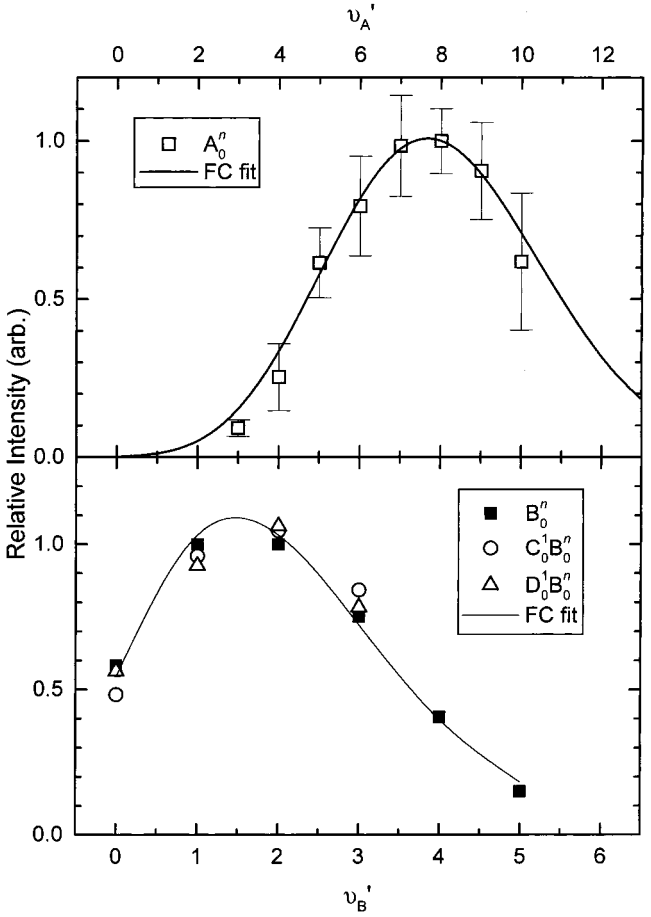

Figure 4. Intensity distributions of the ν_A and ν_B progressions. A one-dimensional Franck−Condon fit with parameters in the text is shown as a solid line through each set of data.

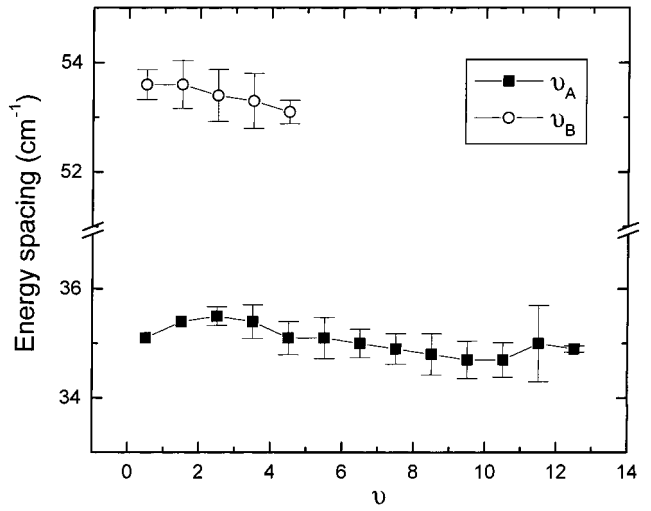

Figure 5. Average energy difference between adjacent members of the ν_A and ν_B progressions as a function of υ_A and υ_B. Points are plotted at the half-integer value of υ between the adjacent members. The error bars are one standard deviation.

distribution δ was kept fixed at 0.934, while D remained unconstrained. Overlaid in Figure 5 is the resultant best FC fit (having the least sum of squares deviation) to the observed intensities. The parameters that produced this fit were $\delta = 0.934$ and $D = 4.0$. The numbering that this analysis produced is the one used in Tables 1 and 2, with the first definite cold band assignment being the A_0^3 transition, and the maximum occurring for A_0^8. The FC analysis is consistent with the assignments

TABLE 3: Spectroscopic and Structural Parameters of 1,2′-BN

	spectroscopic constant	value (cm^{-1} unless stated)	assignment
S_1 state	ν_A'	35.1	torsion
	ν_B'	53.5	butterfly (out of plane)
	ν_C'	60.6	wag (in plane)
	ν_D'	138.1	asymmetric inter-ring mode or naphthalene ring mode
S_0 state	ν_A''	30.5	torsion
	ν_B''	(48)[a]	butterfly (out of plane)
S_1-S_0	T_{00}	30828.2	electronic origin transition
	$\Delta\theta$	18°	change in torsional angle
S_2-S_1	ΔE	800	dimer splitting

[a] estimated from Franck−Condon analysis

in these tables, inasmuch as no peak is assigned a negative value of υ_A. For example, if the FC analysis had provided a numbering of A_0^2 for the first peak of the origin progression, then all transitions in Table 1 would have their υ_A labels reduced by one from those actually listed in the table. The transition assigned as $A_0^0 B_0^3$ would then have had an assignment of $A_0^{-1} B_0^3$, which is of course nonsense. The FC analysis is not definitive; an assignment where all quanta of υ_A are shifted by +1 in Tables 1 and 2 would work, however, the resultant fit to the experimental intensities would be somewhat poorer. Assuming the FC analysis has provided the correct labeling for υ_A is it straightforward to extrapolate back to the origin transition from any of the transitions in Table 1 (assuming harmonic frequencies). This extrapolation provides $T_{00} = 30\,828.2 \pm 0.9$ cm^{-1}, averaged over the 60 observed transitions involving only ν_A and ν_B.

The intensity of the members of the ν_B progression was also fitted to a harmonic, one-dimensional Franck−Condon model. In this case the numbering is secure, however now there is no information on ν_B''. δ was constrained to lie between 0.9 and 1.1, that is allowing a maximum frequency difference between the two electronic states of 20%. D was unconstrained. The data for each of the three different progressions shown in the lower half of Figure 4 are actually the average over all members of the ν_A progressions. For example, the $A_0^6 B_0^n$ progression shown in Figure 2 contributes to the solid squares in Figure 4. However, there are up to 12 other values of υ_A that also contribute to each solid square data point. The best FC fit is also shown in the figure, which required $D = 1.95$ and $\delta = 0.95$. The fit was not particularly sensitive for δ between 0.90 and 1.00, however, the various values of δ did not affect D much, always producing $1.9 < D < 2.0$. A value of $\delta = 0.95$ would require the ground-state frequency, $\nu_B'' = 48$ cm^{-1}, to be smaller than in the excited state, like ν_A. By the same argument as above for ν_A, this is reasonable, for if ν_B is an inter-ring mode, which is almost assured for such a low frequency, then the increased double bond character in the C−C′ bond upon electronic excitation would probably increase the frequency of all inter-ring vibrations.

A summary of the observed vibrational frequencies and tentative assignments can be found in Table 3.

IV. Discussion

In this work, the LIF excitation spectrum of jet-cooled 1,2′-BN has been measured. The spectrum is dominated by many

medium length progressions in two active vibrations, labeled ν_A and ν_B with harmonic vibrational structure spaced 35.1 and 53.5 cm^{-1}, respectively. Two more low-frequency vibrations exhibit short progressions: $\nu_C = 60.6$ cm^{-1} and $\nu_D = 138.1$ cm^{-1}. A Franck−Condon analysis allowed the electronic origin transition to be estimated to be $T_{00} = 30\,828.2$ cm^{-1}.

The conformation of the naphthalene moieties in binaphthyls is very sensitive to the subtle competition between π-conjugation and steric forces. The most recent theoretical modeling of BN structure (both electronic and nuclear) was published over a decade ago using semiempirical methods. One of the primary goals of this work was to explore whether this level of theory captured the essence of this competition or whether our understanding of the binaphthyl systems would benefit from a more detailed theoretical study. One of the key indicators of the competition between π-conjugation and steric forces is the dihedral angle between the naphthalene systems. Below, we estimate this change in dihedral angle. Then, we compare the experimental results with previous theory and with the other isomers of binaphthyl.

A. Torsional Potential and Franck−Condon Analysis. The lowest frequency vibrational mode found in the $S_1 \leftarrow S_0$ LIF spectrum was $\nu_A' = 35.1$ cm^{-1}. This vibration has been tentatively assigned as the torsional vibration by analogy with many other biaryl systems in which the lowest frequency is the torsion (for example biphenyl, 1,1′-BN and 2,2′-BN).[1,2,19,20] The progression in ν_A is quite long, which indicates a substantial change in equilibrium dihedral angle upon electronic excitation. Figure 5 demonstrates that the frequency spacing between ν_A energy levels remains constant at a value of approximately 35 cm^{-1} over the range $\upsilon_A = 0$ to 13. Thus, the torsional potential energy function must be fairly harmonic for at least the first 500 cm^{-1}. Eventually, of course the potential energy function must reach a maximum which represents the barrier to isomerization between the cis and trans forms of 1,2′-BN (see inset, Figure 1). Because in Figure 5 there is no evidence of any change in spacing between levels at higher υ_A', the barrier must be much higher than the 500 cm^{-1} (13 quanta) of the torsional potential observed in this work.

We therefore use a simple harmonic potential to describe the torsion with

$$V(\theta) = {}^1/_2\, k(\delta\theta)^2 \qquad (1)$$

where $\delta\theta$ is the change in dihedral angle from the equilibrium position and k the force constant for torsion about the central C−C′ bond. The force constant is related to the vibrational frequency through the moment of inertia about the C−C′ bond by

$$k = (2\pi c\omega)^2 I \qquad (2)$$

where the reduced momentum of inertia $I = 158$ amu·Å^2 for 1,2′-BN (using the geometry of naphthalene[27]) and $\omega = 30.5$ or 35.1 cm^{-1} for the S_0 and S_1 states of 1,2′-BN, respectively. Thus, $k'' = 4350$ $cm^{-1}rad^{-2}$ and $k' = 5800$ $cm^{-1}rad^{-2}$.

The change in dihedral angle that occurs upon electronic excitation may also be estimated from the torsional potential and the Franck−Condon analysis. The transition with maximum intensity in the progressions occurs at A_0^8. The amplitude of vibration for $\upsilon_A' = 8$ is approximately ±18° derived from the calculated potential function. A simple interpretation of the Franck−Condon principle would then place this angle "vertically above" the ground-state equilibrium geometry, in other words that the change in equilibrium dihedral angle is 18° upon

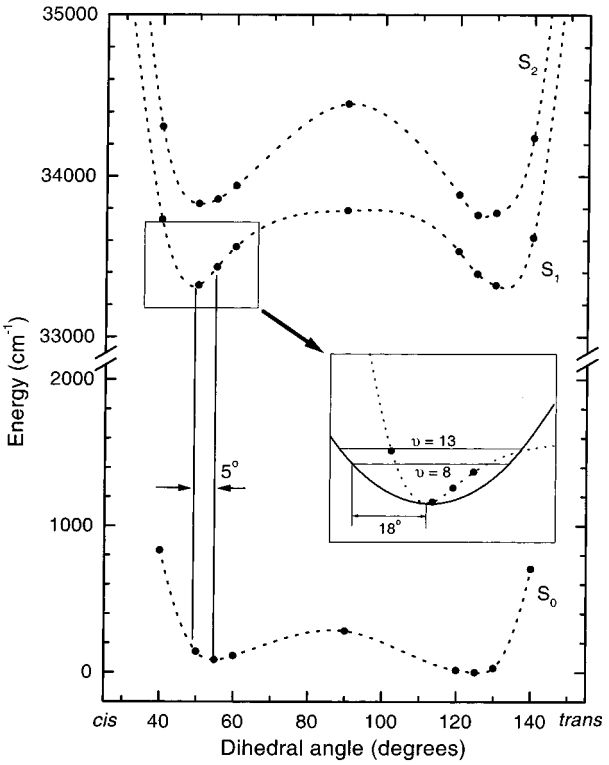

Figure 6. Representation of the potential energy function of S_0, S_1 and S_2 electronic states for rotation about the C−C′ bond. Semiempirical points are from Baraldi[24] and fitted with a spline. The region around the equilibrium geometry of the cis-like conformer in the S_1 state is expanded in the central region and shown in comparison with the harmonic potential derived from these experiments.

electronic excitation. Alternatively, the parameter D in the Franck−Condon analysis is related to the change in normal coordinate between the ground and excited electronic states. The FC fit to the experimental data provided $D = 4.0$, which corresponds approximately ±19° in the change of torsional angle. These two numbers are in good agreement.

B. Comparison with Theory. The theoretical calculations of Baraldi for the three lowest lying electronic states of 1,2′-BN are shown schematically in Figure 6.[24] The $S_1 - S_0$ transition is calculated to be about 33 300 cm^{-1} The two lowest excited states, S_1 and S_2 are quite close in energy, lying only ∼500 cm^{-1} apart. In both these excited states, the electronic excitation is somewhat localized on each naphthalene moiety and the overall molecular orbital can be described as a symmetric and antisymmetric combination of these basis states (the ^1L_b state of each naphthalene). Additionally, the calculations show that the equilibrium geometry of the two rotamers (cis-like and trans-like) lie very close in energy and angle; both being 55−60° from the planar geometries and less than 100 cm^{-1} different in energy in all three states (S_0, S_1, and S_2).

Experimentally, we have observed a series of progressions in two active vibrations with frequencies of 35.1 and 53.5 cm^{-1}, as well as two other sets of progressions based on vibrations with frequencies of 60.6 and 138.1 cm^{-1}. The electronic origin was estimated to be 30 328.2 cm^{-1}, in quite respectable agreement with theory. However, it is reasonable to question at this stage whether the transitions in the spectrum should be attributed to one or both rotamers, and perhaps to either or both of the dimer states, S_1 and S_2. The Deslandres table of Table 1 shows remarkably constant energy level spacings involving ν_A and ν_B. The spacings are the same throughout the table to experimental spectroscopic accuracy and it would seem unlikely

that two different conformers, or two different electronic states would yield frequencies the same to within ± 1 cm^{-1}. The same argument applies to ν_C and ν_D as each of these appears with the same set of ν_A and ν_B progressions, thereby connecting each of these vibrations to the same electronic state and same conformer as ν_A and ν_B.

The semiempirical calculations provide an explanation. The $S_1 - S_0$ transition energies for both the cis-like and trans-like rotamers are less than 100 cm^{-1} different. However, the oscillator strength for the cis-like molecule is about 5−6 times larger than for the trans. Additionally, the $S_1 - S_0$ transition energy is slightly lower for the cis rotamer. For these reasons, we propose that *all* assigned peaks in the spectrum belong to the cis rotamer, and that all belong to the $S_1 - S_0$ transition.

The spectrum in Figure 1 shows another broad peak displaced about 800 cm^{-1} higher than the center of the $S_1 - S_0$ band. The $S_2 - S_0$ transition energy is calculated to lie ∼500 cm^{-1} higher in energy for both cis and trans isomers. The calculated oscillator strength for this transition in both conformers is ∼2/3 that of the $S_1 - S_0$ in the cis conformer. It is therefore reasonable that this broad transition is assigned to the $S_2 - S_0$ transition in one or both conformers.

There are two other points of comparison between the experimental data and the previous calculations; the vibrational frequency of the torsion, and the change in dihedral angle. The inset to Figure 6 shows the semiempirical potential in comparison with the experimentally derived harmonic torsional potential. They are clearly qualitatively different. The theoretical potential has a low-lying barrier to isomerization through 90° between the rotamers and a very steep potential toward 0°. The observed experimental energy levels already exceed the calculated barrier height, and furthermore the energy ladder remains quite harmonic through this region, suggesting that the barrier is quite a lot higher. Figure 6 also demonstrates the small change in dihedral angle (∼5°) that is predicted to occur upon electronic excitation. The experimental change in dihedral angle (based on ν_A being the torsional vibration) is closer to 18°. These two observations indicate that although the semiempirical calculations appear to have predicted the electronic energy reasonably, they have not performed well in representing the electronic energy as a function of dihedral angle.

C. Comparison with other Binaphthyls. 1,2′-BN has received much less attention than its cousins 1,1′-BN and 2,2′-BN. It is obviously of lower symmetry, which makes calculation and spectroscopy more difficult, and its characteristics are believed to lie between 1,1′-BN and 2,2′-BN in most regards. The energy of the S_1 electronic state lies between that for 1,1′-BN and 2,2′-BN.[5,24] 1,1′-BN has a much more perpendicular dihedral geometry; the naphthalene rings are at almost 90° in the S_0 state with a single minimum and displaced a few degrees from perpendicular in the S_1 state (with a double minimum potential).[15,22] As a consequence, the progression in the torsional mode is quite short and quite different for the cis-like and trans-like conformations.[19] In the perpendicular configuration, the dimer coupling between the two naphthalene states is weak causing the splitting to be small (only about 50 cm^{-1}).[19] The electronic transition is also a similar energy to the naphthalene monomer.[19] The conformation of 2,2′-BN is much flatter than any of the other isomers, lying 30° from planar in both cis and trans conformations in the ground state, and completely planar in the excited state.[20,23] This stronger interaction of the naphthalene moieties across the connecting bond lowers the electronic energy.[20] 1,2′-BN lies between its cousins in these regards. The dihedral angle was calculated to be ∼55° from planar in each rotamer, and the electronic energy is intermediate between 1,1′-BN and 2,2′-BN.[24,25]

Although the electronic character of 1,2′-BN is intermediate between the two symmetric counterparts, the spectroscopy is quite different. 1,2′-BN is of course a lower symmetry species than the other two. This results in a more complex spectrum that includes more active progressions. 1,1′-BN and 2,2′-BN show significant FC activity in only one vibration, the torsion. The spectrum of 1,2′-BN, on the other hand, exhibits strong activity in two very low-frequency modes. We have assigned the torsion to the lowest frequency mode and an out-of-plane wag to the second lowest frequency; however, this assignment is somewhat arbitrary and based more on historical and intuitive grounds. The reason that we are expressing this caveat here is that, unlike in the symmetric binaphthyls, a local mode torsion around the C−C′ bond cannot be a normal mode of vibration for 1,2′-BN. Simple examination of the molecule in the inset to Figure 1 shows that rotation about this bond will lead to significant displacement of the center-of-mass, and therefore, the torsion motion may be kinetically coupled to some form of out-of-plane wag to keep the center-of-mass fixed. This will have the effect of confusing the comparison between theory and experiment as the theory is plotting the energetics of a local mode displacement (about the C−C′ bond), whereas the experiment is measuring a normal mode displacement, which conceivably might contain significant contributions from several local modes.

In summary, there are aspects of the spectroscopy of 1,2′-BN and indeed all three BNs that are quite well understood in terms of both the prevailing semiempirical theory of binaphthyl being a weakly coupled naphthalene dimer. The theory seems to work best for 1,1′-BN, where the naphthalenes are in an almost perpendicular configuration, and hence, the coupling between them is weak. The agreement between theory and experiment is poorer for 1,2′-BN and 2,2′-BN, where the naphthalenes are more planar; especially for 2,2′-BN, where the theory predicts a dihedral angle of 30° in the excited state, whereas the experiment confirms the molecule is planar. Perhaps the largest discrepancy, however, is the form of the torsional potential. The semiempirical excited state potentials seem to be qualitatively different to that suggested by the experimental data; the equilibrium geometry is different and the barrier height for change in conformation from one conformer to the other is far too low in 1,2′-BN.

To answer the above questions we are undertaking ab initio calculations of the electronic and nuclear configurations of all three BN isomers, in both the ground and first excited electronic states. For the present 1,2′-BN work, we seek to confirm whether the lowest frequency vibration is indeed the torsion, whether there is any other reason that we could observe a spectrum attributable to only one conformer, and whether the ab initio torsional potential fits the experimental energy levels better. In doing so, we hope to gain a better understanding of π-conjugation effects in this prototypical biaryl system.

Acknowledgment. The financial support of the Australian Research Council is gratefully acknowledged. We wish to thank Dr. George Bacskay for discussions regarding theoretical aspects of this work. F. Z. acknowledges a PhD stipend from the School of Chemistry.

References and Notes

(1) Ito, M. *J. Phys. Chem.* **1987**, *91*, 517.
(2) Takei, Y.; Yamaguchi, T.; Osamura, Y.; Fuke, K.; Kaya, K. *J. Phys. Chem.* **1988**, *92*, 577.

(3) Drucker, R. P.; McClain, W. M. *Chem. Phys. Lett.* **1974**, *28*, 255.
(4) Gamba, A.; Rusconi, E.; Simonetta, M. *Tetrahedron* **1970**, *26*, 871.
(5) Friedel, R. A.; Orchin, M.; Reggel, M. *J. Am. Chem. Soc.* **1948**, *70*, 199.
(6) Chakraborty, T.; Lim, E. C. *J. Chem. Phys.* **1993**, *98*, 836.
(7) Dekkers, J. J.; Hoornweg, G. P.; MacLean, C.; Velthorst, N. H. *J. Mol. Spec.* **1977**, *68*, 56.
(8) Layton, E. M. J. *J. Mol. Spec.* **1960**, *5*, 181.
(9) Werst, D. W.; Brearley, A. M.; Gentry, W. R.; Barbara, P. F. *J. Am. Chem. Soc.* **1987**, *109*, 32.
(10) Finley, J. P.; Cable, J. R. *J. Phys. Chem.* **1993**, *97*, 4595.
(11) Laane, J. *J. Phys. Chem. A* **2000**, *104*, 7715.
(12) Hara, Y.; Nicol, M. F. *Bull. Chem. Soc. Jpn.* **1978**, *51*, 1985.
(13) Hochstrasser, R. M. *Can. J. Chem.* **1961**, *39*, 459.
(14) Lacey, A. R.; Craven, F. J. *Chem. Phys. Lett.* **1986**, *126*, 588.
(15) Riley, M. J.; Lacey, A. R.; Sceats, M. G.; Gilbert, R. G. *Chem. Phys.* **1982**, *72*, 83.
(16) Tetreau, C. *J. Phys. Chem.* **1986**, *90*, 4993.
(17) Post, M. F. M.; Eweg, J. K.; Langelaar, J.; Voorst, J. D. W. V.; Maten, G. T. *Chem. Phys.* **1976**, *14*, 165.
(18) Gustav, K.; Suhnel, J.; Wild, U. P. *Chem. Phys.* **1978**, *31*, 59.
(19) Jonkman, H. T.; Wiersma, D. A. *J. Chem. Phys.* **1984**, *81*, 1573.
(20) Del Riccio, J. R.; Zhang, F.; Lacey, A. R.; Kable, S. H. *J. Phys. Chem.* **2000**, *104*, 7442.
(21) Jonkman, H. T.; Wiersma, D. A. *Chem. Phys. Lett.* **1983**, *97*, 261.
(22) Baraldi, I.; Ponterini, G.; Momicchioli, F. *J. Chem. Soc, Faraday Trans. 2* **1987**, *83*, 2139.
(23) Baraldi, I.; Bruni, M. C.; Caselli, M.; Ponterini, G. *J. Chem. Soc., Faraday Trans. 2* **1989**, *85*, 65.
(24) Baraldi, I. *J. Chem. Soc., Faraday Trans. 2* **1989**, *85*, 839.
(25) Ciolowski, J.; Pisskorz, P.; Liu, G.; Moncrieff, D. *J. Phys. Chem.* **1996**, *100*, 19 333.
(26) Henderson, J. R.; Muramoto, M.; Willett, R. A. *J. Chem. Phys.* **1964**, *41*, 580.
(27) Craig, D. P.; Hollas, J. M. *Philos. Trans. R. Soc. London* **1961**, *253*, 569.